Smart Sounding Table Using Adaptive Neuro-Fuzzy Inference System

Osman Ünal
Sakarya University of Applied Sciences, Department of Mechanical Engineering, Sakarya, Turkey,
osmanunal@subu.edu.tr

Nuri Akkaş
Sakarya University of Applied Sciences, Department of Mechanical Engineering, Sakarya, Turkey

Smart Sounding Table Using Adaptive Neuro-Fuzzy Inference System

Osman Ünal*, Nuri Akkaş

Sakarya University of Applied Sciences, Department of Mechanical Engineering, Sakarya, Turkey

Abstract

Marine engineers measure the liquid level (sounding depth) to calculate the volumetric content of a ship's tank. The sounding depth is determined using an ullage pipe located at specific points on the tanks. To estimate the accurate volume of liquid, considering the ship's trim and heel conditions, engineers use a tank table (sounding table) consisting of hundreds of pages. However, this method is time-consuming and lacks intermediate values for sounding depth, trim, and heel. Ship designers recommend to use linear interpolation for intermediate values, yet this process is also time-consuming. This paper proposes the implementation of an Adaptive Neuro-Fuzzy Inference System (ANFIS) to digitize the sounding table. To our knowledge, we are the first to apply the ANFIS method to develop a model for liquid volume in non-uniform geometric tanks, accounting for different trim and heel conditions of the vessel. In this study, the digitization of the sounding table using ANFIS is referred to as the Smart Sounding Table (SST). SST's accuracy is validated against experimental values, revealing an R-squared value of 0.9999, a mean absolute percentage error of 0.3515, and a root mean square error of 0.0366. These metrics clearly show that the SST algorithm accurately and reliably models experimental data. Marine engineers input three parameters (sounding depth, trim, and heel) into the SST, enabling rapid and accurate determination of liquid volume in their tanks, without the need for interpolation or exhaustive page searches.

Keywords: Marine engineers, Marine vessels, Sounding table, ANFIS

1. Introduction

Accurate, precise, and reliable measurements of liquid volume in tanks are essential for the global fair trading of commercial liquids, the safe discharge and loading of flammable petroleum products to prevent catastrophic accidents, safe storage of hazardous waste oil, and the environmentally sound release of blackwater (toilet water) and greywater (bath water) into the sea [1,2]. Liquid volumes within stationary land-based tanks are determined based on liquid height. When the tank's geometry is uniform, calculating the amount of liquid is straightforward. However, for tanks with non-uniform geometric shapes, the liquid volume is determined using an incremental table correlating volume with liquid height—referred to as tank calibration charts, tank tables, or sounding tables [3]. Numerous methods exist in the literature for generating tank calibration tables, including the volumetric [4,5], geometric [6,7], laser scanning [8,9], and Monte Carlo [10,11] approaches. The volumetric approach, also known as the liquid calibration method, involves filling the non-uniformly shaped tank with a known volume of calibration liquid to determine the liquid height within the tank [12]. This process is repeated at specific intervals, generating a calibration table that shows the liquid volume corresponding to incremental increases in liquid height at specific intervals [13]. The liquid height is measured at a predetermined point in the tank for each volume increment. Water is typically used as the calibration liquid owing to its low cost. Despite

* Corresponding author.
E-mail address: osmanunal@subu.edu.tr (O. Ünal).

its cost-effectiveness, the volumetric approach has certain drawbacks [14]:

- Time expenditure: Depending on tank dimensions, the tank calibration process typically takes 4−5 h. This leads to significant time losses for operational processes, especially when many tanks require calibration.
- Labor requirement: Calibration requires at least two engineers or metrology specialists.
- Water consumption: The calibration process requires the addition of water to the tank, resulting in substantial water usage.

Conversely, the geometric method is preferred by many tank designers because it has several advantages such as time efficiency (calibration typically takes 15−20 min), mitigation of wastewater concerns, and the ability for a single specialist to conduct the tank calibration [15].

With technological advancements, the laser scanning method has evolved as a means of measuring tank capacity. Researchers often prefer to use the laser scanning method owing to its simplicity and ability to determine tank capacity with acceptable errors [16−18]. The laser scanning method employs laser light emission to assess the internal volume of the tank. Laser scanning encompasses both external and internal scanning. External scanning involves measurements taken with the laser scanner placed outside the tank, avoiding potential interference from external environmental obstacles. In internal scanning, the tank's capacity is measured by positioning the laser scanner inside the tank, provided the tank's bottom remains constant [19].

The Monte Carlo method has been developed to efficiently measure tank capacity while minimizing costs. Being an effective approach, it is widely adopted by researchers, similar to the laser scanning method [20−22]. When utilizing the Monte Carlo method for tank capacity measurement, the process involves several steps. First, sensor points are identified on the inner surface of the tank. Subsequently, using the sensor point locations and the distances between each point along the tank surface, a decision criterion is established to generate sample points. According to this criterion, the number of sample points at different heights is calculated. Lastly, the number of sample points and the corresponding capacitance values linked to different liquid levels are determined. This methodology enables the most efficient determination of tank capacity while utilizing a minimal number of samples and experiments [23].

The process of tank calibration is important for ship designers. However, they do not distribute tank calibration charts as digital data; instead, they provide marine engineers with only a sounding table book. This sounding table book, comprising hundreds of pages, causes substantial time loss when engineers need to calculate tank volumes. Furthermore, owing to its prolonged use in the engine room over the years, the sounding book may become worn, soiled, and torn. In this study, we propose to digitize the sounding table using the Adaptive Neuro-Fuzzy Inference System (ANFIS) technique, aimed at streamlining marine engineers' tasks. ANFIS, a subset of artificial neural networks, combines neural networks and fuzzy logic [24,25]. Its wide application stems from its ability to solve strongly non-linear real-world problems, leveraging the strengths of both neural networks and fuzzy logic [26−30]. In contrast to stationary land-based tanks, the calculation of liquid volume in marine tanks is influenced not only by the liquid level's height but also by the vessel's position and inclination. The determination of liquid volume relies on three input parameters—depth, heel, and trim. Consequently, creating a model for the tank calibration chart of marine vessels is difficult, given its highly non-linear nature. Therefore, in this study, we use the ANFIS technique to model the sounding table. The digitization of the tank sounding table for marine vessels using the ANFIS technique is the novelty and main contribution of this paper. Marine engineers can input the three parameters (sounding depth, trim, and heel) into the proposed novel model, enabling them to immediately obtain the liquid volume in the tanks without resorting to interpolation or searching through hundreds of pages.

2. Sounding table

Marine engineers measure the ullage or sounding depths to calculate the liquid content within the tanks of marine vessels. Sounding depth refers to the liquid height, and ullage depth is determined by subtracting the sounding depth from the total tank height. Fig. 1 shows both ullage and sounding depths.

The advantage of determining ullage depth is that it is an easier measurement that minimizes contamination of the sounding measuring equipment suspended from the top of the tank when the tank is nearly full with a viscous fluid such as crude oil.

Unlike stationary tanks on land, tanks on ships can experience inclinations to the starboard (right)
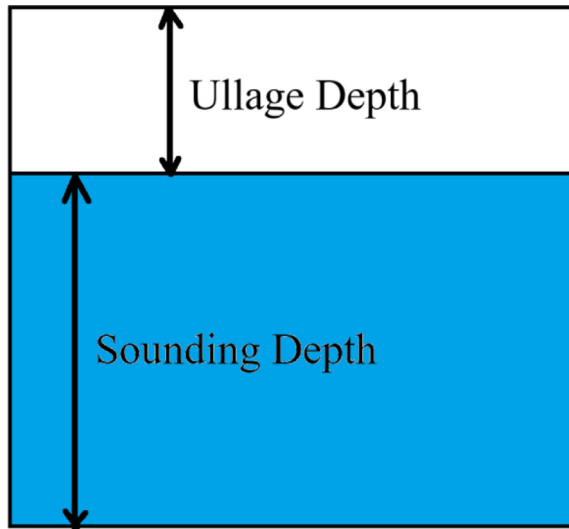
Fig. 1. Ullage and sounding depths.

or port (left) sides, as well as fore (forward) or aft (backward), depending on the ship's orientation. Thus, marine engineers must calculate the liquid volume within the tanks when the ship inclines in these directions. Because the fluid quantity in the tanks is determined based on the liquid height, this height will vary with the ship's inclination. In such situations, marine engineers use correction tables to calculate the amount of liquid inside the tanks. The sounding table includes both the heel and trim correction tables. The heel correction table is used to correct the liquid level (sounding depth) for the starboard or port inclination of the vessel. Meanwhile, the trim correction table is used to determine the liquid volume based on the vessel's inclination towards the stem (fore) or stern (aft). The usage of the sounding table can be summarized in the following steps:

#Step 1. Determine three input parameters: the liquid height within the tank, the vessel's heel, and the vessel's trim. For this example, let us assume that marine engineers measured the ullage depth of the liquid to be 1518 cm. The total height of the tank is 1822.8 cm, indicating a sounding depth of 304.8 cm (1822.8 − 1518 = 304.8). The ship's heel is −1° (a negative value implies that the vessel is tilted to the port side), and the ship's trim is 2 m by the stern (indicating an inclination of the vessel towards the back).

#Step 2. Use the heel correction table

Table 1 shows an example of a heel correction table used for tanks in a marine vessel. Negative corrections signify an inclination towards the port side, while positive values indicate an inclination towards the starboard side, both measured in degrees. For example, if the ship tilts by 1° to the port side, an ullage depth of 1518 cm should be adjusted as 1518 − 4 = 1514 cm. This corrected value (1514 cm) must be used in the trim correction table to determine the liquid content.

If the ship is not inclined to either port or starboard, the heel correction table is not used, and the liquid volume can be directly derived by inputting the value of 1518 cm into the trim correction table.

#Step 3. Use the trim correction table to determine the liquid volume in cubic meters

In Step 2, the ullage depth was determined to be 1514 cm after heel correction. The point of intersection for the 1514 cm ullage depth and a stern trim of 2 m yields a value of 47.10 m³.

The trim correction table encompasses three scenarios. Even keel denotes a situation where there is no inclination through the fore and aft directions of the ship. Trim by stem (1 m) signifies that the ship's fore descends into the sea by an additional meter compared to the aft. Because the propeller must be submerged in the water, marine vessels are usually designed as stern-inclined. Therefore, only one meter is considered for trim by stem in Table 2. Finally, trim by stern denotes how much deeper the ship's aft sinks compared to the fore. All volumes specified in the trim correction table are in cubic meters.

These three steps clearly show that determining liquid volume using the sounding table is a time-consuming process. Both heel and trim correction

Table 1. Heel correction table (The heel correction determined in Step 2 is highlighted in bold).

Ullage Depth (cm)	Sounding Depth (cm)	Heel by Port (degree)				Heel by Starboard (degree)			
		−4	−3	−2	−1	1	2	3	4
1516	306.8	−15.9	−11.9	−8.0	−4.0	4.0	8.0	11.9	15.9
1518	**304.8**	**−15.8**	**−11.9**	**−7.9**	**−4.0**	**4.0**	**7.9**	**11.9**	**15.8**
1520	302.8	−15.7	−11.8	−7.9	−3.9	3.9	7.9	11.8	15.7
1522	300.8	−15.6	−11.7	−7.8	−3.9	3.9	7.8	11.7	15.6
1524	298.8	−15.5	−11.7	−7.8	−3.9	3.9	7.8	11.7	15.5
1526	296.8	−15.4	−11.6	−7.7	−3.9	3.9	7.7	11.6	15.4
1528	294.8	−15.3	−11.5	−7.7	−3.8	3.8	7.7	11.5	15.3
1530	292.8	−15.2	−11.4	−7.6	−3.8	3.8	7.6	11.4	15.2

Table 2. Trim correction table (The trim correction determined in Step 3 is highlighted in bold).

Ullage Depth (cm)	Sounding Depth (cm)	Trim by Stem 1 m	Even Keel	Trim by Stern (meter)			
				1	2	3	4
1510	312.8	48.18	48.09	48.01	47.92	47.83	47.75
1512	310.8	47.77	47.68	47.60	47.51	47.43	47.34
1514	**308.8**	**47.36**	**47.27**	**47.19**	**47.10**	**47.02**	**46.93**
1516	306.8	46.95	46.87	46.78	46.70	46.61	46.53
1518	304.8	46.55	46.46	46.38	46.29	46.21	46.12
1520	302.8	46.14	46.06	45.97	45.89	45.80	45.72
1522	300.8	45.74	45.65	45.57	45.49	45.40	45.32
1524	298.8	45.34	45.25	45.17	45.08	45.00	44.92

table must be taken into account. Furthermore, these correction tables do not include intermediate values. For example, an ullage depth of 1513 cm is not provided in the trim correction table. To address this, ship designers advise using interpolation for such intermediate values. However, interpolation in the heel and trim correction tables is time-consuming. Marine engineers are required to monitor the liquid quantities in numerous tanks daily, which entails performing multiple interpolations for each tank using the heel and trim correction tables. This issue leads to a considerable time inefficiency. In this study, we propose to digitize the sounding table using ANFIS, aiming to improve time efficiency. Moreover, the digitization model developed in this study can potentially be integrated with real-time tank level monitoring systems [31−36] interfaced with the computer in the cargo operation room on the ship. This setup would enable instantaneous and continuous determination of the fluid volume within each tank on the ship, utilizing the ship's trim and heel data.

3. Adaptive Neuro-Fuzzy inference system

The Adaptive Neuro-Fuzzy Inference System (ANFIS), first developed in 1993, is a hybrid predictive model that leverages both neural network [37] and fuzzy logic [38] to establish mapping relationships between inputs and outputs. The fuzzy logic system possesses learning capabilities, while the neural network operates as a comprehensive interpreter. ANFIS effectively uses these features to construct accurate models [39]. The preliminary data is passed through a set of constraints to decrease the optimization search space using the fuzzy system, and the adaptation of previous propagations to the designed network is performed by the neural networks to control the fuzzy parametric values.

The purpose of the fuzzy inference system is to establish a proper relationship between input and output parameters using fuzzy logic. ANFIS, being a sub-branch of adaptive networks, is functionally related to fuzzy inference systems. Therefore, ANFIS is a suitable technique for mapping strongly non-linear relationships between multiple input and output parameters [40]. In this study, there are three input variables (sounding depth, heel, and trim) and one output (liquid volume). Because each input parameter has two membership functions, there are a total of eight rules ($2^3 = 8$). The schematic of the ANFIS structure in the MATLAB environment is shown in Fig. 2.

ANFIS structure contains five layers: fuzzification, product, normalization, defuzzification, and output.

Layer 1: Fuzzification of input variables using membership functions

In the ANFIS structure of the projection welding model, a, b, and c are the input parameters denoting sounding depth, heel, and trim, respectively. A_1, A_2, B_1, B_2, C_1, and C_2 are the fuzzy variables that can be calculated using the following equations. In equations (1)−(3), μ values are the membership functions of each fuzzy variable.

$$A_i = \mu_{Ai}(a), i = 1, 2 \tag{1}$$
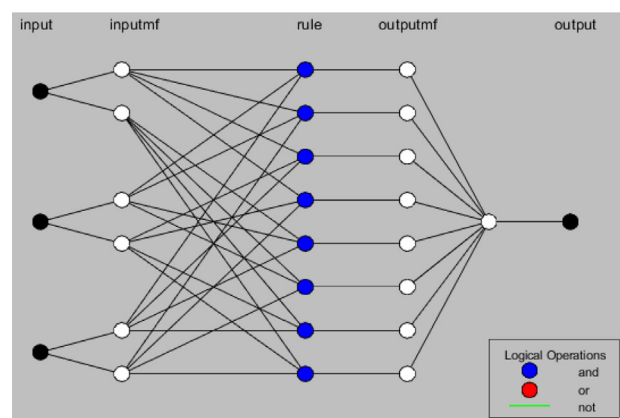
$$B_i = \mu_{Bi}(b), i = 1, 2 \tag{2}$$

Fig. 2. ANFIS structure in the MATLAB environment.

$$C_i = \mu_{Ci}(c), i = 1, 2 \tag{3}$$

Equation (4) shows an example calculation of membership functions for the fuzzy variables A, depicted as a bell-shaped function. In equation (4), $\{k_i, l_i, m_i\}$ represent the antecedent or premise parameters for each membership function.

$$\mu_{Ai}(a) = \frac{1}{1 + \left[\left(\frac{a - m_i}{k_i}\right)\right]^{l_i}} \quad i = 1, 2 \tag{4}$$

Layer 2: Incentive strength of each rule

The incentive strength of rules can be calculated using the following equation:

$$W_i = \mu_{Ai}(a) \times \mu_{Bi}(b) \times \mu_{Ci}(c), i = 1, 2 \tag{5}$$

Layer 3: Normalizing the firing or incentive strengths

This layer can be described as the ratio of the incentive strength of each rule to the sum of all the rules' incentive strengths. Equation (6) shows the calculation process for normalization.

$$\overline{W_i} = \frac{W_i}{\sum_i W_i}, i = 1, 2 \tag{6}$$

Layer 4: Defuzzification

This layer represents the output of each rule and can be expressed using the following equation. In equation (7), $\{\alpha, \beta, \gamma, \theta\}$ can be determined through the least square method.

$$\overline{W_i}.f_i = \overline{W_i}.(\alpha_i.a + \beta.b + \gamma_i.c + \theta_i) \tag{7}$$

Layer 5: Final output

The overall output of all incoming signals is calculated using equation (8).

$$\sum_i \overline{W_i}.f_i = \frac{\sum_i W_i.f_i}{\sum_i W_i}, i = 1, 2 \tag{8}$$

Equation (8) represents the liquid volume as the output of all processes. Fig. 3 shows the general structure of ANFIS. As a result of these processes, the relationship between the three inputs (depth, heel, and trim) and the output (tank volume) is modeled by the ANFIS method, which is a combination of fuzzy logic and artificial neural networks. In Fig. 3, the symbols "Ullage Depth," "Heel," and "Trim" represent the input layer, while the symbol "Volume" represents the output layer. The remaining symbols represent intermediate layers and serve as coefficients used to determine the correct relationship between the input values and the output value. After these coefficients are determined using fuzzy logic, the model is finalized.

The sounding depth range is limited from 0 to 214 cm, while the heel range is from −4 to +4°. The trim range is from −1 to +4 m. Fifty percent of the values in the sounding table were used for generating and training the ANFIS model. These values were used to determine coefficients for intermediate layers. The remaining 50% of the data was used to test the ANFIS model. Both training and test data are significant. A large set of training data enhances the quality of the model, while a large set of test data ensures that the reliability of the model is accurately controlled. Upon validation using the test data, it was determined that the ANFIS model was 99.9% compatible with the test data.

4. Results and discussion

In this section, an ANFIS-based model was developed using the heel and trim correction charts in the sounding table. By inputting the depth, heel, and trim values into this model, the liquid volume in the tank can be quickly calculated in a digital environment. While improving this model, named Smart Sounding Table (SST), a subset of 324 data entries out of the total 648 in the sounding table was reserved to test the accuracy of the model. The SST model was trained using the remaining 324 data entries. Subsequently, the test data and the responses generated by the SST model were compared. Four most popular evaluation metrics in the literature [41−43] were used to determine the quality of the SST model: the coefficient of determination (R^2), the mean absolute error (MAE), the mean absolute percentage error (MAPE, %), and the root mean squared error (RMSE).

In the literature, the coefficient of determination quantifies the degree of compatibility between the developed model and the original data. It assumes values from zero to one. If the coefficient of determination equals to zero, the model does not predict the original data. When the coefficient of determination is between zero and one, the model partially predicts the original data. If the coefficient of determination is one, the model accurately predicts the original data [44]. Equation (9) shows the formula for the coefficient of determination:

$$R^2 = \frac{\sum_{i=1}^{n}(y_i - f_i)^2}{\sum_{i=1}^{n}(y_i - \overline{y})^2} \tag{9}$$

In equation (9), y_i denotes each original value, f_i represents the estimated value obtained from the SST model, $\overline{y}$ represents the average value of the original data, and n is the number of measurements. The coefficient of determination for the SST model
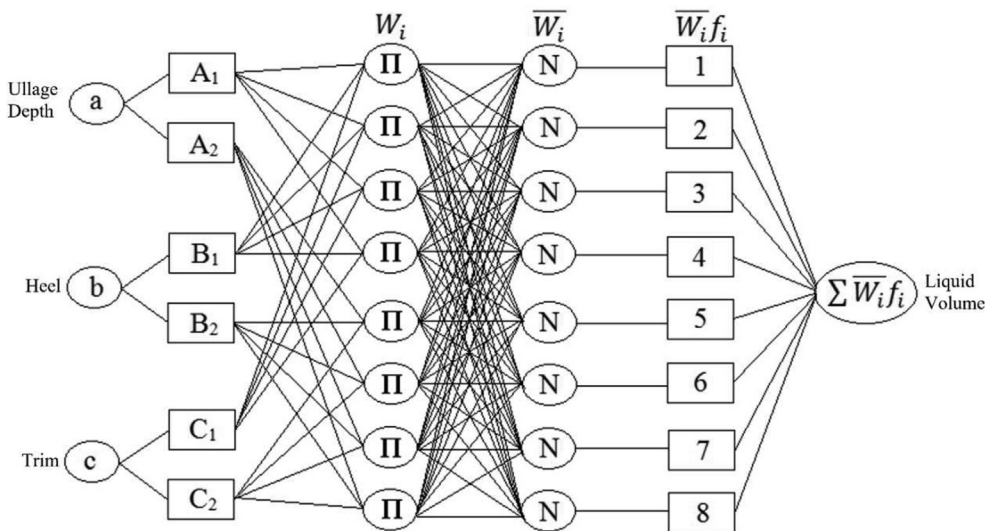
Fig. 3. ANFIS architecture.

was investigated based on both the 324 training data entries and the 324 test data entries. The calculated R^2 values for the training dataset and the test dataset were 0.999994670878718 and 0.999978034438207, respectively. In general, a coefficient of determination value greater than 0.99 indicates a good relationship between the predicted and actual results [45].

Absolute error is the amount of error in measurements, expressed as the difference between the responses of the developed model and the actual values. The mean absolute error is the average of all absolute errors. The accuracy of a forecasting system is determined using the mean absolute percentage error, also referred to as the mean absolute percentage deviation. When the units of the variable are scaled to percentage units, facilitating comprehension, the mean absolute percentage error is the most frequently used metric for anticipating errors. The lowest possible mean absolute percentage error is 0, which corresponds to a perfect prediction. The formulas used to calculate the mean absolute error and the mean absolute percentage error are provided in equations (10) and (11) [46,47]:

$$MAE = \frac{1}{n}\sum_{i=1}^{n}\left(y_i - f_i\right) \tag{10}$$

$$MAPE = \frac{1}{n}\sum_{i=1}^{n}\left(\frac{y_i - f_i}{y_i}\right) \tag{11}$$

The mean absolute errors were calculated as 0.0217 m³ and 0.0299 m³ based on the training and test datasets, respectively. Considering the tank's approximate capacity of 50 cubic meters, a volume error less than 0.03 cubic meters is within reasonable limits. An error of 0.06% clearly indicates that the model fits well with the real data. The mean absolute percentage errors are 0.3515% for the training dataset and 0.4829% for the test dataset. These errors, both under 0.5%, are insignificant.

The root mean square error is the square root of the mean squared error resulting from the difference between the actual and estimated data. It measures the distribution of residuals, serving as an indicator of how far the developed model is from the original data. When the value approaches zero, the data are concentrated around the prediction model. Equation (12) shows the formula of the root mean square error [48]:

$$RMSE = \sqrt{\frac{1}{n}\sum_{i=1}^{n}\left(y_i - f_i\right)^2} \tag{12}$$

According to equation (12), the root mean square errors calculated from the training and test data were 0.0366 and 0.0747, respectively. The obtained results clearly show that the deviation of the responses of the improved SST model from the original data is negligibly small. These results indicate that the SST model and the actual dataset (sounding table) are in agreement. To more clearly show the compatibility of the improved SST model with the test data, Table 3 was created by randomly

Table 3. 25 randomly selected original data entries and responses of SST.

Data from the Sounding Table (m^3)	Responses of SST (m^3)	Percentage Error (%)
8.3340	8.3533	0.2316
22.1000	22.0909	0.0412
16.5990	16.5923	0.0404
25.5820	25.5989	0.0661
41.7240	41.7019	0.0530
26.9740	26.9766	0.0096
21.4270	21.4165	0.0490
2.5940	2.5807	0.5127
26.6740	26.6754	0.0052
45.3470	45.3445	0.0055
41.5700	41.5712	0.0029
8.3340	8.3533	0.2316
20.8640	20.8492	0.0709
12.1830	12.2093	0.2159
44.0770	44.0772	0.0005
4.5140	4.5252	0.2481
36.4950	36.4607	0.0940
3.3590	3.3842	0.7502
2.8620	2.8478	0.4962
17.5750	17.5876	0.0717
19.0330	19.0411	0.0426
18.3000	18.3225	0.1230
35.5000	35.4614	0.1087
3.2170	3.2431	0.8113
18.3000	18.3225	0.1230

selecting 25 data entries from 324 test data entries. Table 3 includes the 25 randomly chosen test data entries, the responses of the SST model, and the percentage error for each data entry. According to Table 3, the maximum percentage error across these 25 test data entries is less than 1%. This implies that the developed SST model is compatible with the original data.

After validating the developed SST model using the actual dataset obtained from the sounding table book, a three-dimensional graph of the SST 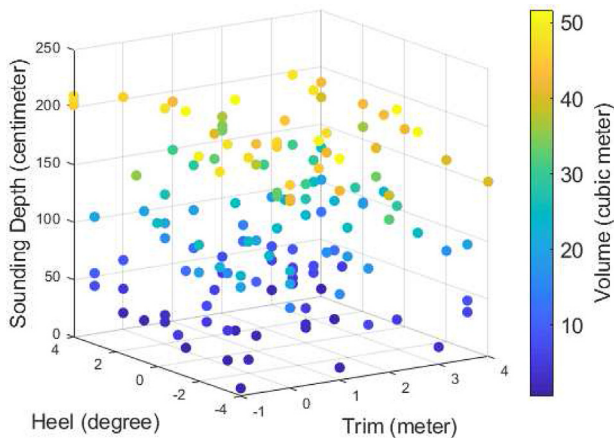model was generated (Fig. 4). The SST model is a continuous function with three inputs and one output. The input parameters of this model are a depth ranging from 0 to 214 cm, a heel varying from −4 to +4°, and a trim ranging from −1 to +4 m. In the developed SST model, any value in the abovementioned range can be selected as an input parameter. The SST model outputs the volume in cubic meters corresponding to these three input parameters. Fig. 4 shows the volume values derived from the insertion of 150 randomly selected depth, heel, and trim values into the SST model. The color of the circles in Fig. 4 represents the volume values.

5. Conclusion

In this study, the frequently used sounding table book, comprising numerous pages, was digitized using ANFIS. To our knowledge, we are the first to apply the ANFIS method for constructing a model that computes the liquid volume within non-uniform geometric tanks under varying trim and heel conditions of the vessel. The developed model has three inputs (depth, heel, and trim) and a single output (liquid volume). Using the improved model (SST), marine engineers will be able to determine the liquid quantity in the tanks by inputting the values for depth, heel, and trim, without the need for interpolating or searching through hundreds of book pages. The SST model presented in this paper was validated using the four most commonly used evaluation metrics in the literature. R^2, MAE, MAPE, and RMSE were calculated as 0.99, less than 0.03, less than 0.5%, and less than 0.075, respectively. These evaluation metrics clearly show that the responses of the SST model and the actual data are in agreement. SST can be applied to any tank model on any ship. The MATLAB code required for SST modeling is provided in the Appendix. The Appendix also provides a link to Google Drive containing a section of the sounding table book from an actual ship and the code pertinent to the SST model. Using this code, marine engineers can develop their own SST models for their tanks, thereby saving time while on the ship. In the future, the SST model can be integrated with the real-time level measurement equipment aboard the vessel. This real-time measurement capability could ensure the continuous and instantaneous accurate measurement of tank volume.

Conflict of interest

The authors declare that there are no conflicts of interest regarding the publication of this paper.

Fig. 4. 3D responses of the SST model.

Appendices

Appendix A. Trim correction table

```
clc,clearvars,close all
%Trim Correction Table
data=xlsread('data1'); [m,n]=size(data); tr=1:2:m-1; te=2:2:m;
testData=data(te,:); pdata=data; pdata(te,:)=[]; trainingData=pdata;
clear pdata
options = anfisOptions('InitialFIS',[10 10],'EpochNumber',1000,'ValidationData',testData);
[fis,trainError,stepSize,chkFIS,chkError]=anfis(trainingData,options);
writefis(fis,'fs1');
```

Appendix B. Heel correction table

```
clc,clearvars,close all
%Heel Correction Table
data=xlsread('data2'); [m,n]=size(data); tr=1:2:m-1; te=2:2:m;
testData=data(te,:); pdata=data; pdata(te,:)=[]; trainingData=pdata;
clear pdata
options = anfisOptions('InitialFIS',[10 10],'EpochNumber',1000, 'ValidationData',testData);
[fis,trainError,stepSize,chkFIS,chkError]=anfis(trainingData,options);
writefis(fis,'fs2');
```

Appendix C. Smart sounding table

```
function v=sst(depth,heel,trim)
%Smart Sounding Table
fis1=readfis('fs1'); fis2=readfis('fs2'); depth=depth+evalfis([depth,heel],fis1);
if depth<0; depth=0; end
if depth>214; depth=214; end
v=evalfis([depth,trim],fis2);
end
```

Appendix D. Plot solution

```
Clc,clearvars,close all
dpth=randi([0,214],150,1); hl=randi([-4,4],150,1); trm=randi([-1,4],150,1); v=sst(dpth,hl,trm);
scatter3(trm,hl,dpth,50,v,'filled')
view(-34, 14)
xlabel('Trim (meter)','FontSize',14)
ylabel('Heel (degree)','FontSize',14); ylim([-4 4])
zlabel('Sounding Depth (centimeter)','FontSize',14)
c=colorbar;
c.Label.String='Volume (cubic meter)';
c.FontSize=14;
set(gcf,'color','w');
```

Appendix E. Google drive link

https://drive.google.com/drive/folders/1CEKeWkZb8oFoc1VxrlIqhNljXYE3hEOM?usp=sharing

References

[1] Meškuotienė A, Kaškonas P, Raudienė E, Dobilienė J, Urbonavičius BG. Calibration periodicity of fuel tanks assigned to legal–industrial metrology: A case study. Sustainability 2022;14(16):9817.

[2] Agboola OO, Ikubanni PP, Ibikunle RA, Adediran AA, Ogunsemi BT. Generation of calibration charts for horizontal petroleum storage tanks using Microsoft Excel. MAPAN 2017;32(4):321–7.

[3] Aguilar-Mamani JJ, Villegas-Arroyo Z. Model for optimization of error and uncertainty in the generation of calibration charts for horizontal storage tank. J Phys Conf 2021;1826(1): 012080.

[4] Agboola OO, Akinnuli BO, Akintunde MA, Ikubanni PP, Adeleke AA. Comparative analysis of manual strapping method (MSM) and electro-optical distance ranging (EODR) method of tank calibration. J Phys Conf 2019;1378(2):022062.

[5] Knyva V, Knyva M. Influence of 3D scanning data scattering to volume measurement of horizontal fuel tanks. Elektronika ir Elektrotechnika 2014;20(5).

[6] Wang J, Jintao W, Xiang L, Jingyue Z, Lin T, Ligong G, et al. WALL-climbing robot system for volume calibration of Large Vertical Storage Tank. MAPAN 2023;38(2):295–306.

[7] Nosach VV, Belyaev BM. The calibration of large vertical cylindrical tanks by a geometrical method. Meas Tech 2002; 45(11):1153–7.

[8] Chen X, Xu Y, Wang Y, Wu Z, Chen J, Shi H, Xu Z. Research and verification of internal and external measurement methods of large oil storage tanks capacity based on 3D lasers canning. In: E3S web of conferences. vol. 245. EDP Sciences; 2021. p. 1053.

[9] Chen X, Wu Z, Shi H, Hao H, Chen J, Shen Z. Research on the Application of Three-Dimensional Laser Scanner Method for Whole Life Cycle Capacity Measurement and Safety Monitoring of Storage Tanks. In: 2021 IEEE 15th international conference on electronic measurement & instruments (ICEMI). IEEE; 2021. p. 64–8.

[10] Chen G, Wan Y, Lin H, Hu H, Liu G, Peng Y. Vertical tank capacity measurement based on Monte Carlo method. PLoS One 2021;16(4):e0250207.

[11] Chen G, Hu H, Lin H, Chen L, Wan Y, Xiao T, Peng Y. Research on Capacity Measurement Method of Horizontal Cylindrical Tank Based on Monte Carlo Method. Chem Technol Fuels Oils 2022;58(1):84–9.

[12] Patel S, Parrott B, Abdellatif F, Trigui H. Custody Transfer Tank Calibration Technology. In: Abu Dhabi international petroleum exhibition & conference. OnePetro; 2020.

[13] Papadopoulos K, Tzetzis D, Oancea G, Kyratsis P. Reverse Engineering of a Milk Tank and Evaluation of Volume Metering Procedure. Acad J Manuf Eng 2016;14(1).

[14] Knyva M, Knyva V, Nakutis Ž, Dumbrava V, Saunoris M. A concept of fuel tank calibration process automation within IOT Infrastructure. MAPAN 2016;32(1):7–15.

[15] Knyva M, Knyva V, Meškuotienė A, Kuzas P, Gailius D, Nakutis Ž. 3D laser scanning Pointcloud processing uncertainty estimation for fuel tank volume calibration. MAPAN 2020;35(3):333–41.

[16] Huadong H, Xianlei C, Haolei S, Xuemin L, Pengju Y. The automatic measurement system of large vertical storage tank volume based on 3D laser scanning principle. In: 2017 13th IEEE international conference on electronic measurement & instruments (ICEMI). IEEE; 2017. p. 211–6.

[17] Knyva V, Knyva M, Rainys J. New approach to calibration of vertical fuel tanks. Elektronika ir Elektrotechnika 2013;19(8): 37–40.

[18] Wang J, Liu Z, Tong L, Zhang L, Guo L, Bao X. The non-contact precision measurement and noise reduction method for liquid volume metrology. In: Seventh international symposium on precision engineering measurements and instrumentation. SPIE. vol. 8321; 2011. p. 789–95.

[19] Huadong H, Xianlei C, Haolei S, Xuemin L, Pengju Y. The automatic measurement system of large vertical storage tank volume based on 3D laser scanning principle. In: 2017 13th IEEE international conference on electronic measurement & instruments (ICEMI). IEEE; 2017. p. 211–6.

[20] Chen G, Xiao T, Yan Y, Wan Y, Hu H, Lin H, Peng Y. Influence of Measurement Parameters on the Accuracy of

Determining the Capacity of a Vertical Tank. Chem Technol Fuels Oils 2022;58(1):122—30.

[21] Zhou Y, Lu Z, Cheng K, Yun W. A Bayesian Monte Carlo-based method for efficient computation of global sensitivity indices. Mech Syst Signal Process 2019;117:498—516.

[22] Chaudhury AN, Ghosal A. Determination of workspace volume of parallel manipulators using monte carlo method. In: Computational kinematics: proceedings of the 7th international workshop on computational kinematics that was held at futuroscope-poitiers, France. Springer International Publishing; 2018. p. 323—30.

[23] Chen G, Lin H, Hu H, Yan Y, Wan Y, Xiao T, Peng Y. Research on the measurement of ship's tank capacity based on the Monte Carlo method. Chem Technol Fuels Oils 2022; 58(1):232—6.

[24] Walia N, Kumar S, Singh H. A survey on applications of adaptive Neuro Fuzzy Inference System. Int J Hospit Inf Technol 2015;8(11):343—50.

[25] Tavoosi J, Suratgar AA, Menhaj MB. Stable anfis2 for nonlinear system identification. Neurocomputing 2016;182: 235—46.

[26] Parhi DR, Kundu S. Navigational strategy for underwater mobile robot based on Adaptive Neuro-Fuzzy inference system model embedded with shuffled frog leaping algorithm—based hybrid learning approach. Proc IME M J Eng Marit Environ 2017;231(4):844—62.

[27] Karaboga D, Kaya E. Adaptive network based Fuzzy Inference System (ANFIS) training approaches: A comprehensive survey. Artif Intell Rev 2018;52(4):2263—93.

[28] Chou C-C, Lin K-S. A fuzzy neural network combined with technical indicators and its application to Baltic Dry index forecasting. J Marine Eng Technol 2018;18(2):82—91.

[29] Al-qaness MAA, Ewees AA, Fan H, Abualigah L, Elaziz MA. Boosted ANFIS model using augmented marine predator algorithm with mutation operators for wind power forecasting. Appl Energy 2022;314:118851.

[30] Abdullah SF, Mamat R. Application of swarm intelligence for dynamic properties of moored floating structures using two-dimensional fluid dynamic program. In: Proceedings of the institution of mechanical engineers, Part M: journal of engineering for the maritime environment; 2023. p. 147509022211435.

[31] Liu F, Wang L, Zhang J, Fu Z, Li X, Lv Z, Zhu L. A Real-Time Closed Tank Capacity Measurement Method for Liquid Volume Supporting the Internet of Things, Big Data and Intelligent Ship Supply Chain. In: 2022 international conference on industrial IoT, big data and supply chain (IIoTBDSC). IEEE; 2022. p. 311—6.

[32] Liu Jiangli J, Gong Shangjun, Zhang Lei, et al. Application of multisensor fusion technology in ship liquid level monitoring. Ship Scie Technol 2021;43(6):6.

[33] Wang Xiaoling J. Design of high-precision liquid level telemetry and control system for ships. Commun World 2019;26(5):262—3.

[34] Song Yongqiang J, Zhou Hualiang, Wang HouWei, et al. Analysis of FPSO level telemetry system. Ship Elect Power Technol 2022;42(8):3.

[35] Yan Wei J. Saab. Tank radar level telemetry system management and fault handling. J Wuhan Shipbuild Inst 2022; 21(1):8—15.

[36] Luo Li J. Level telemetry system installation and debugging analysis. J Marine Eng 2020;42(SI). 391-393+465.

[37] Chiu inn-Tong, Fang Chih-Chung. Soft computing technologies in design of fuzzy controller for active vibration isolation systems. J Mar Sci Technol 2016;24(3). Article 17.

[38] Jang J-SR. ANFIS: Adaptive-network-based Fuzzy Inference System. IEEE Transact Syst Man Cybernet 1993;23(3):665—85.

[39] Bhatia M, Ahanger TA, Manocha A. Artificial intelligence based real-time earthquake prediction. Eng Appl Artif Intell 2023;120:105856.

[40] Kazemi MA, Pa M, Uddin MN, Rezakazemi M. Adaptive Neuro-Fuzzy inference system based data interpolation for particle image velocimetry in fluid flow applications. Eng Appl Artif Intell 2023;119:105723.

[41] Al Fuhaid AF, Alanazi H. Prediction of Chloride Diffusion Coefficient in Concrete Modified with Supplementary Cementitious Materials Using Machine Learning Algorithms. Materials 2023;16(3):1277.

[42] Alghamdi A. A hybrid method for big data analysis using fuzzy clustering, feature selection and Adaptive Neuro-Fuzzy inferences system techniques: case of Mecca and Medina hotels in Saudi Arabia. Arabian J Sci Eng 2023;48(2): 1693—714.

[43] Zereg S, Belouz K. Modeling daily reference evapotranspiration using SVR machine learning algorithm with limited meteorological data in Dar-el-Beidha, Algeria. Acta Geophys 2023:1—17.

[44] Nnaji PC, Anadebe VC, Agu C, Ezemagu IG, Ohanehi AA, Onukwuli OD, Eluno EE. Statistical computation and artificial neural algorithm modelling for the treatment of dye wastewater using mucuna sloanei as coagulant and study of the generated sludge. Result Eng 2023:101216.

[45] Agor CD, Mbadike EM, Alaneme GU. Evaluation of sisal fiber and aluminum waste concrete blend for sustainable construction using Adaptive Neuro-Fuzzy inference system. Sci Rep 2023;13(1):2814.

[46] Çağöl G, Güler SN, Ünlü A, Böyükdibi Ö, Tüccar G. Comparative analysis of Multiple linear Regression (MLR) and Adaptive Network-Based fuzzy Inference Systems (ANFIS) methods for vibration prediction of a diesel engine containing NH3 additive. Fuel 2023;350:128686.

[47] Ghasemi M, Samadi M, Soleimanian E, Chau KW. A comparative study of black-box and white-box data-driven methods to predict landfill leachate permeability. Environ Monit Assess 2023;195(7):862.

[48] Oladipo S, Sun Y. Enhanced Adaptive Neuro-Fuzzy inference system using genetic algorithm: a case study in predicting electricity consumption. SN Appl Sci 2023;5(7):186.